

OBTAINING THE CRITICAL SHEAR CRACK KINEMATICS FROM A MULTI-ACTION MODEL AND THE GRG METHOD

Gilcyvania Costa, PUC-Rio, Brazil, gilcyvania@gmail.com

Claudia Campos, Fluminense Federal University, Brazil, cmocampos@id.uff.br

Daniel Cardoso, PUC-Rio, Brazil, dctcardoso@puc-rio.br

ABSTRACT

The behavior of concrete structures subjected to shear forces is a challenging topic for the scientific community. It involves the contribution of several shear force transfer mechanisms, such as aggregate interlock, dowel action, residual concrete tension, and uncracked concrete zone. The contribution and interaction between these mechanisms are dependent on the shape and kinematics of the critical shear crack. Such crack characteristics are influenced by the structural system and materials that compose the element. The prediction models have not considered all the mechanisms and have been mostly applied in reinforced concrete structures with steel bars. Therefore, this paper presents a multi-action model in which the referred mechanisms of shear force are also considered in the equilibrium of forces and moments, with the kinematics of the critical shear crack obtained from an optimization process using the GRG method. Numerical results of crack opening-slip, contribution of the transfer mechanisms, and values of critical rotation and neutral axis depth in the failure stage of the beam are presented.

KEYWORDS

Critical shear crack; GRG Method; Shear force mechanisms.

INTRODUCTION

The shear behavior of a concrete beam is a complex and challenging subject, as it is influenced by the interaction of several shear force transfer mechanisms that develop and contribute to the ultimate resistance. The shear force transfer occurs through the aggregate interlock, the residual tensile strength of concrete, the dowel action at longitudinal reinforcement, and the uncracked concrete zone. In a comprehensive model, the presence of normal stresses due to bending must also be considered.

In the context, several studies (Baumann & Rusch, 1970; Fenwick & Paulay, 1968; H.P.J. Taylor, 1974; T. Paulay & P.J. Loeber, 1974; Walraven, 1980) conducted since the 1960s have aimed to identify the contributing actions at the shear failure. These studies have defined influential parameters and consistent models to individually assess the transfer mechanisms with reasonable accuracy. However, the impact of each mechanism is strongly influenced by the shape and the kinematics of the shear crack (Cavagnis, 2017) and, therefore, they should be computed using models which are in agreement with the shape in the critical stage.

Due to the difficulty in monitoring shear crack formation and evolution, the main design guidelines provide shear capacity predictions based on empirical formulations that do not consider the kinematics in the critical stage. Furthermore, the design expressions depend on the test conditions for which they were developed. The tests are usually aimed at the evaluation of traditional reinforced concrete beams with steel bars.

In recent years, the scientific community's focus has been on studying shear behavior from the perspective of closely monitoring the relative shear displacements (opening and sliding) occurring within the crack with greater precision. This has been made possible by the advancement of monitoring techniques, such as Digital Image Correlation (DIC), which have enabled more comprehensive and

detailed experimental research on the shear crack in its most critical stage (Cavagnis, 2017; Gomes et al., 2023; Resende, 2020).

From the use of more reliable data available in the literature, comprehensive predictive models can be formulated and rigorously validated. For this purpose, the models should be able to adequately represent the shape and kinematics of the shear crack. Furthermore, it is desirable for these predictive models to be independent of empirical parameters, capturing the behavior of beams made from new materials, such as Fiber Reinforced Concrete (FRC) and Fiber Reinforced Polymer (FRP) bars.

In this regard, mechanics-based models have attracted the interest of researchers as these may be used to address the aforementioned issues and simplified when necessary to obtain practical design expressions. Among the models proposed through the years, noteworthy examples include the models of Reineck (1991), the Critical Shear Crack Theory (CSCT) by Muttoni et al. (Campana et al., 2013; Fernández Ruiz & Muttoni, 2008; Muttoni & Fernández Ruiz, 2008; Muttoni & Schwartz, 1991) and, more recently, the model based on the Shear Crack Propagation Theory (SCPT) proposed by Classen (2020).

The Reineck mechanical model (1991) is based on the truss analogy and assumes a linear shape for the shear crack, neglecting the sliding between crack surfaces. Furthermore, the Reineck model (1991) only considers two shear force transfer mechanisms: the dowel action and the aggregate interlock. On the other hand, the mechanical model proposed by Muttoni et al. (Campana et al., 2013; Fernández Ruiz & Muttoni, 2008; Muttoni & Fernández Ruiz, 2008; Muttoni & Schwartz, 1991), based on CSCT, has achieved great visibility in the scientific community. It employs a bilinear crack shape that accounts for the crack kinematics by considering the crack opening measured at a critical depth. Thus, this model incorporates the evaluation of aggregate interlock using the model proposed by Walraven (1980), as well as the contribution by dowel action. Lastly, the mechanical model proposed by Classen (2020) considers the contribution of resistant forces and moments, addressing various shear force transfer mechanisms and crack propagation as the loading evolves. Although this model is comprehensive and mechanically consistent, it approximates the shape of the shear crack as bilinear.

In this context, this present study proposes a multi-action mechanical model that incorporates the aforementioned contributing actions based on models specifically designed to represent each action individually. The model defines the shear capacity of statically determinate concrete beams using an arbitrary shape for the critical crack. The main advantage of the proposed model is the prediction of the critical crack kinematics, which is determined by parameters such as the neutral axis depth and the critical rotation that lead a beam to shear failure. Additionally, the model can quantify the corresponding contribution of each mechanism at the failure.

The proposed mechanical model is developed using the Object-Oriented Programming (OOP) paradigm in the MATLAB (MATrix LABoratory) development environment. Once the model is formulated, an optimization algorithm based on the Generalized Reduced Gradient (GRG) method is employed using the package available in the Microsoft Excel solver. The results obtained are presented through an application to a reinforced concrete beam with FRP bars.

Shear force transfer mechanisms

The proposed prediction model incorporates the transfer mechanisms given from individual models available in the literature. The adopted models have been validated and tested in previous work (Gomes et al., 2023), showing suitability for the purpose of this study.

Aggregate interlock

The stress transfer through aggregate interlock has been represented from several empirical-based models, such as those proposed by Bazant & Gambarova (1980) and Walraven & Reinhardt (1981),

and semi-empirical-based models, highlighting the two-phase ones, proposed by Walraven (1980), and the contact density model, proposed by Li et al. (1989).

The Li et al. (1989) model considers that stress transfer between crack surfaces occurs through contact units (dA_θ). The contact unit represents a unit area on the surface, which has a slope θ . The model formulation involves a function, called the contact density function $\Omega(\theta)$, which represents the probabilistic distribution of the contact inclination angles θ of the rough surface in the crack plane.

Based on experimental data, Li et al. (1989) fitted a function $\Omega(\theta) = 0.5\cos(\theta)$ and defined a valid model for concretes below 50 MPa, given by the following expressions:

$$\sigma = m \left[\frac{\pi}{2} - \cot^{-1}\varphi - \frac{\varphi}{1+\varphi^2} \right] \quad \text{Eq. 1}$$

$$\tau = m \left(\frac{\varphi^2}{1+\varphi^2} \right) \quad \text{Eq. 2}$$

where $\varphi = \delta/w$, $m = 3,83f_c^{1/3}$, with f_c being the concrete compressive strength.

Therefore, in this study, Li et al. (1989) model will be adopted to represent the aggregate interlock according to the expressions presented.

Dowel action

Among the several models available in the literature to represent the dowel action (Baumann & Rusch, 1970; Resende, 2020; Vintzēleou & Tassios, 1986), the one developed by Cavagnis et al. (2018b, 2018a) will be adopted in this study. In this model, the contribution of the dowel force V_d is dependent on the specific strain of the bar ε_r at the location of the reinforcement layer, which is related to parameters regarding the splitting crack formation. Thus, the variables associated with the splitting crack are: effective width b_{ef} on which the effective tensile stresses $f_{ct,ef}$ relative to each bar act, and the effective length l_{ef} , which corresponds to the section where the pullout force is transferred to the concrete.

$$V_d = n f_{ct,ef} b_{ef} l_{ef} \quad \text{Eq. 3}$$

where

$$f_{ct,ef} = k_b f_{ct} \quad \text{Eq. 4}$$

$$b_{ef} = \min \left\{ \left(\frac{b}{n} - \phi_b \right); 4c; 6\phi_b \right\} \quad \text{Eq. 5}$$

$$l_{ef} = 2\phi_b \quad \text{Eq. 6}$$

where n is the number of bars; f_{ct} is the tensile strength of concrete; b is the section width; ϕ_b is the bar diameter; c is the reinforcement cover; and k_b is a reduction factor that depends on the bar strain ε_r and should always be lower than or equal to 1.

$$k_b = 0.063 \left(\frac{1}{\varepsilon_r} \right)^{0.25} \quad \text{Eq. 7}$$

The strain ε_r can be estimated by Eq. 8, where Δh is the bar horizontal deformation, due to the opening of the shear crack, and the value of l_b (tributary length), at which contributing cracks develop to the critical shear crack (Eq. 9), is defined according to experimental observations (Cavagnis et al., 2018b).

$$\varepsilon_r = \frac{\Delta h}{l_b} \quad \text{Eq. 8}$$

$$l_b = |d - d_{NA}| \quad \text{Eq. 9}$$

In the previous equation, d is the section effective depth and d_{NA} is the neutral axis depth.

Concrete residual tensile strength

The residual tensile stresses in concrete can be represented from tensile stress-crack opening law (Hillerborg, A.; Modeer, 1976; Hillerborg, 1980). This type of law represents the stress transfer that occurs in a crack by means of the aggregate bridge mechanism. A crack consists of the Fracture Processing Zone (FPZ), located near the crack tip and which is also responsible for the crack mouth opening displacements. In fiber-reinforced concrete, in the crack also occurs the stress transfer via fiber bridge mechanism (Hillerborg, 1980).

Thus, the characteristic behavior of stress-crack opening can be obtained through direct tensile tests or indirect tests, such as four-point bending, with the aid of an inverse analysis to determine the parameters of the fracture law.

In this work, in the absence of characterization tests, the bilinear model suggested by the Model Code 2010 (FIB, 2014) was used, according to equation (10).

$$\sigma_{ct}(w) = \begin{cases} f_{ct} \left(1 - 0,8 \frac{w}{w_1}\right), & w \leq w_1 \\ f_{ct} \left(0,25 - 0,05 \frac{w}{w_1}\right), & w_1 < w \leq w_{\max} \\ 0, & w \geq w_{\max} \end{cases} \quad \text{Eq. 10}$$

where $w_1 = G_f/f_{ct}$ and $\alpha_1 = 0,2$; G_f is the fracture energy of concrete and w_{\max} is the maximum crack width, both obtained as suggested.

Shear transferred through the uncracked concrete zone

The uncracked concrete zone has its shear force transfer capacity dependent on the location of the critical shear crack, being represented by the section above this crack. Consequently, the shear force can be obtained by the integration of shear stresses along this zone, as proposed by Mörsh (1909), considering linear elastic concrete and disregarding the tensile in concrete. Besides that, more recently, a model proposed by Lopez et al. (2021) and Cavagnis et al. (2018a) has been satisfactorily employed (Gomes et al., 2023). In this work, this proposal will be adopted to represent the shear contribution given by the uncracked concrete zone.

According to Lopez et al. (2021), the stress distribution in the compressed concrete is considered linear elastic. In addition, the hypothesis that the uncracked concrete zone coincides with the neutral axis depth d_{NA} is adopted. Therefore, the tensile stresses in the uncracked concrete are neglected. Thus, by obtaining the compressive normal force N_{uncr} in the section, the shear portion V_{uncr} can be obtained from the inclination α of the compressive strut (Gomes et al., 2023), as shown in the following equation and Figure 1.

$$V_{uncr} = N_{uncr} \tan(\alpha) = \sigma_c c_{m2} b \left(\frac{h_t}{3} - \frac{c_{m2}}{2}\right) \frac{1}{r_t} \quad \text{Eq. 11}$$

In Figure 1, the parameters c_{m2} , h_t and r_t are identified. In Lopez et al. (2021), the values of σ_c and c_{m2} are adopted as the compressive strength of concrete and the effective depth of the stress block, i.e., $0,8d_{NA}$.

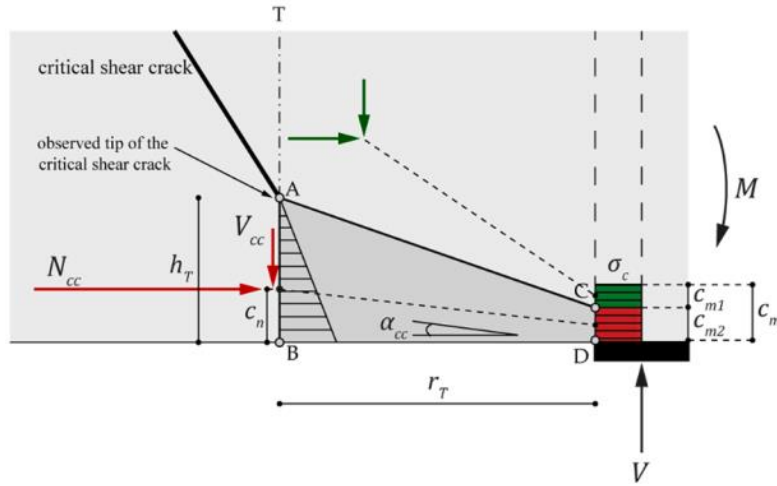


Figure 1: model idealization by Lopez et al. (2021).

Normal transferred by concrete and by FRP reinforcement

In order to make the proposed model consistent and comprehensive, the equilibrium conditions should also consider the normal compressive and tensile forces in the concrete, as well as the tensile force in the longitudinal reinforcement of the beam. For these contributions, the Hognestad classical model (1955) is adopted for the compressive concrete, while a linear elastic behavior is assumed for the tensile concrete and the tensile FRP longitudinal reinforcement. Moreover, the contribution of the tension-stiffening effect is incorporated in the reinforcement contribution from the model presented by Costa & Cardoso (2023).

PROPOSED MODEL

The actual kinematics of the critical shear crack leads to a more accurate prediction of the shear force transfer mechanisms, resulting in a reliable shear strength response and helping to understand the isolated impact of these mechanisms on the beam global behavior. In recent years, models available in the literature have assumed simplified formats, such as linear or bilinear, to represent the shear crack (Classen, 2020; Marí et al., 2015; Muttoni & Fernández Ruiz, 2008). These simpler formats can result in an unrealistic kinematics, leading to inaccurate responses. Accordingly, in order to determine the shear strength and the contribution of actions in reinforced concrete beams, the proposed model presents a strategy to determine the shear crack critical kinematics. This is possible by adopting a nonlinear function $f(x)$ to represent the shape of the crack.

A priori, a statically determinate structural system is defined, and then a relationship between bending moment and shear is established. This relationship is necessary to address the equilibrium requirements of the model. In this study, the adopted structural system corresponds to a beam subject to a concentrated loading (Figure 2). In Figure 2a, an arbitrary function $f(x)$ is presented for contextualization purposes. Note that the chosen function should approximately fit to the shape of the inclined shear crack, since in this proposed model, the splitting crack is not considered. The crack real shape presented in Figure 2b was obtained from test results in literature (Resende, 2020). Figure 2a also shows the critical section of analysis, defined based on the shear span a . Moreover, L is the total length of the beam, while b and d are its base and effective depth, respectively.

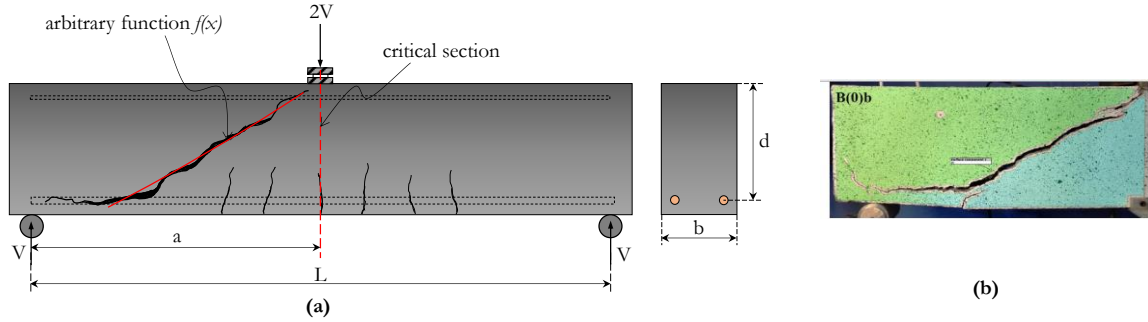


Figure 2: (a) structural system adopted; (b) experimental critical crack – adapted (Resende, 2020).

For the adopted structural system, the moment-shear relationship is given by Eq. 12, with λ equals a/d .

$$M_r = V_r \lambda d \quad \text{Eq. 12}$$

Critical kinematics

From an established crack function, a critical kinematics (w and δ) for this crack must be obtained to evaluate the contributing actions and determine the resistant capacity of the section. The kinematics can be obtained from the solution of a nonlinear equations system, which will be presented later.

This equations system is solved based on an optimization algorithm to obtain the optimum values of θ and d_{NA} corresponding to the defined shape. These obtained values lead to the equilibrium of normal forces N on the section and satisfy the relationship between the resistant moment M_r and the resistant shear V_r on the section (Eq. 12). Hence, the critical kinematics is obtained, resulting in the resistant capacity of the section (V_r, M_r).

The shear crack critical kinematics represents how much the formed crack faces will open (w_i) and slide (δ_i) according to rotation θ given at the crack tip. Each integration point i , whose coordinates are x_i, y_i , moves assuming a new position after rotation, with the new coordinates being x'_i, y'_i . The points coordinates, before and after of the rotation, determine the upper and lower faces of the crack, respectively (Figure 3). The new coordinates are obtained from the following equations, where x_{cr} and y_{cr} are the coordinates of the crack tip.

$$x'_i = (x_i - x_{cr})\cos\theta - (y_i - y_{cr})\sin\theta + x_{cr} \quad \text{Eq. 13}$$

$$y'_i = (x_i - x_{cr})\sin\theta + (y_i - y_{cr})\cos\theta + y_{cr} \quad \text{Eq. 14}$$

Based on the coordinates of the upper and lower crack contours, the opening and slip are obtained geometrically.

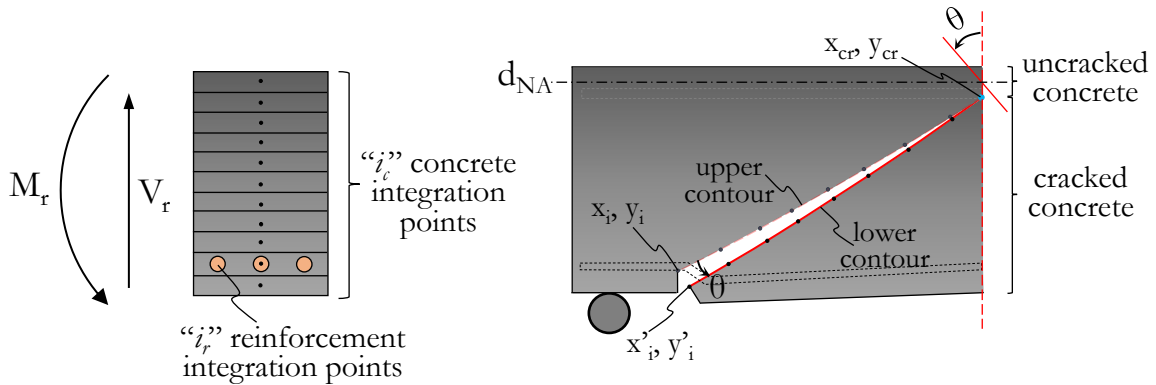


Figure 3: discretized section and crack with the identification of the upper and lower crack contours, as well as the cracked and uncracked sections.

Evaluating of the mechanisms

From the determined function $f(x)$ and the location of the crack tip (Figure 3), the transfer actions can be evaluated at each integration point i . The integration points are given by the discretized concrete layers (i_c) and the reinforcement layers (i_r).

For the points outside the crack, the strains ε_i in the materials are calculated at each point, with distance d_i from the section top to the analysis point i . The values of ε_i are obtained from Eq. 15, which depend on the θ and d_{NA} . From this, the normal forces (N_i) and tangential forces (V_i) at each point pertaining to the uncracked zone are determined from the models presented previously. Meanwhile, for the points inside the crack, the forces N_i and V_i are calculated from the mechanisms acting in the crack, which depend on the kinematics obtained.

$$\varepsilon_i = \frac{2\theta(d_{NA}-d_i)}{a} \quad \text{Eq. 15}$$

Force equilibrium equations and problem constraints

The equilibrium conditions must be satisfied considering the resistant forces described previously. In the following table, a summary of the normal and tangential forces obtained from the numerical integration of stresses along the section and the critical crack is presented. In the table, the indices “*uncr*”, “*ai*”, “*rt*”, “*r*”, and “*da*” refer to the resultant forces due to the uncracked concrete zone, the aggregate interlock, the residual concrete tension, the reinforcement and the dowel action, respectively. Figure 4 presents these forces acting on the section and the crack, with their respective lever arms z , as well as to the external forces N_e , V_e and moment M_e , with $N_e = 0$. The lever arms are necessary for the equilibrium of moments in the reinforcement and are obtained geometrically, since the points coordinates are known.

Table 1: resistant resultant forces

Resistant resultant forces

Concrete normal (N_{unc})
Concrete shear (V_{uncr})
Aggregate interlock normal (N_{ai})
Aggregate interlock shear (V_{ai})
Residual tensile concrete normal (N_{rt})
Residual tensile concrete shear (V_{rt})
Reinforcement tensile (N_r)
Dowel action shear (V_{da})

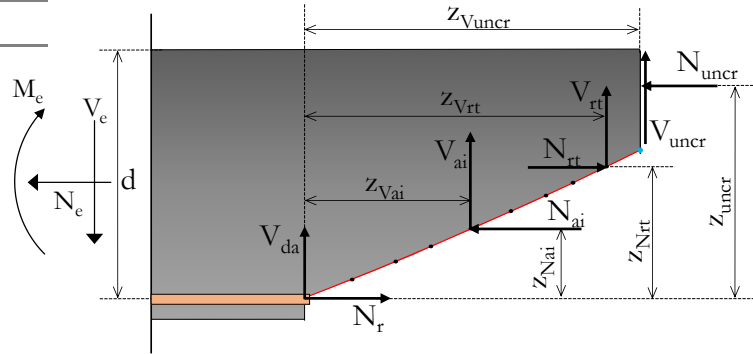


Figure 4: resultant forces and lever arms

Thus, the equilibrium equations for normal, shear and moment are presented below, being possible to obtain the resistant shear V_r from Eq. 17.

$$\sum H = 0 \therefore N_r - N_{uncr} - N_{ai} + N_{rt} - N_e = 0 \quad \text{Eq. 16}$$

$$\sum V = 0 \therefore V_{ai} + V_{da} + V_{rt} + V_{uncr} - V_e = 0 \quad \text{Eq. 17}$$

$$\sum M = 0 \therefore N_{uncr}z_{N_{uncr}} + V_{uncr}z_{V_{uncr}} - N_{rt}z_{N_{rt}}$$

$$+V_{rt}z_{V_{rt}} + N_{ai}z_{N_{ai}} + V_{ai}z_{V_{ai}} - M_{ext} = 0 \quad \text{Eq. 18}$$

The expression of V_r , obtained from Eq. 17, can be replaced in Eq. 12, defining the Eq. 19. Thus, this equation must be satisfied since the moment is obtained in Eq. 18.

$$M_r = (V_{ai} + V_{da} + V_{rt} + V_{uncr})\lambda d \quad \text{Eq. 19}$$

GRG method and the nonlinear equations system solution

The definition of the critical kinematics is given by obtaining the values of the critical rotation θ_{cr} and the neutral axis depth d_{NA} , determined by an optimization algorithm. Once the mechanical problem presented above has been formulated, an optimization process is used to determine the solution of the nonlinear equations system formed by equations 16 and 19, as shown below:

$$\begin{cases} R_1(d_{NA}, \theta) = N_r - N_{uncr} - N_{ai} + N_{rt} = 0 \\ R_2(d_{NA}, \theta) = M_r - (V_{ai} + V_{da} + V_{rt} + V_{uncr})\lambda d = 0 \end{cases} \quad \text{Eq. 20}$$

The solution of the system (Eq. 20) is given by minimizing the objective function F given by Eq. 21, where d_{NA} and θ are the design variables.

$$F(d_{NA}, \theta) = R_1^2 + R_2^2 \quad \text{Eq. 21}$$

Obtaining the optimal variables for the objective function (Eq. 21) was possible from an optimization algorithm based on the Generalized Reduced Gradient (GRG) method. This method, proposed by Abadie and Carpentier (1965), was reformulated and implemented by Lasdon et al. (1974;1978) and it is known for presenting efficient results for several types of nonlinear problems (Sacoman, 2021).

The GRG method unifies the reduced gradient method and the method of Lagrange multipliers. The method incorporates equality constraints into the objective function of the problem by means of Lagrange multipliers, which act as weights, leading to a penalized objective function. The gradient is calculated in a simplified form from the reduced gradient method. In cases formed by inequality constraints, the method incorporates the projected gradient method. The solution is conducted by adjusting the Lagrange multipliers and the design variables at each iteration until the optimal solution is obtained.

This method was adopted in this work due to the nonlinear nature of the objective function. In addition, the exposed problem has nonlinear inequality constraints ($\theta > 0$). Thus, with the objective function in Eq. 21 and the constraint function formulated, the GRG implemented in the Microsoft Excel optimization package can be employed, leading to the answers presented in the application of the next section.

APPLICATIONS AND VALIDATIONS

An application problem is described below based on the tests performed by Gomes et al. (2023), a reinforced concrete beam with Glass Fiber Reinforced Polymers (GFRP) bars, according to the structural system presented in Figure 5a. In Figure 5b, it is possible to observe the crack shape adopted in this study.

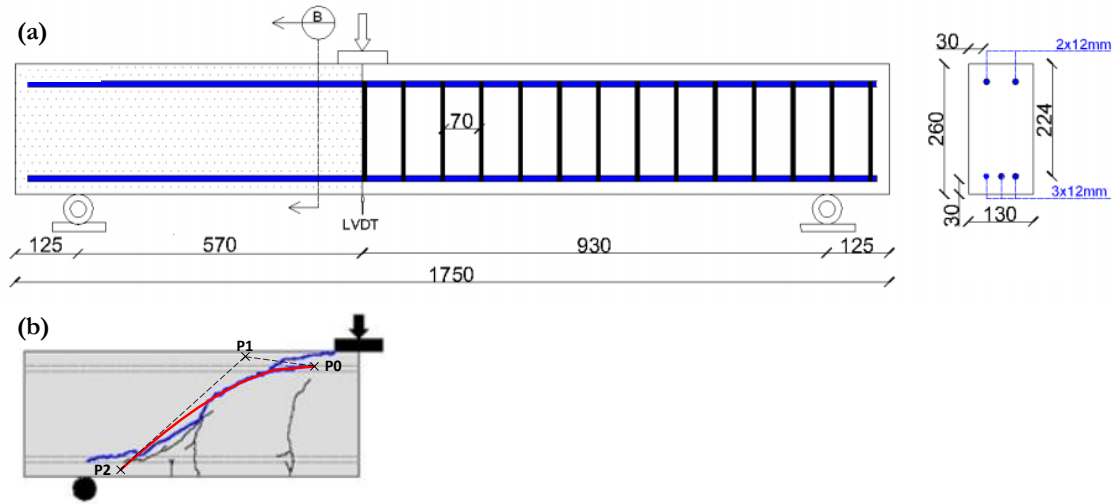


Figure 5: beam setup (Gomes et al., 2023) and established format by a quadratic bezier.

The established shape was given by a quadratic bezier, with control points P0 (102, 30); P1 (240, 10); and P2 (490, 238). The quadratic bezier was chosen because it is a parametric representation curve, with useful properties for this application, such as maintaining its shape even after rotations are applied. Parametric representations of curves are interesting because they can efficiently deal with complex shapes, like implicit representations, and can be described with low computational cost, like explicit representations.

The concrete adopted in this study had a compressive strength $f_{ck} = 40.8$ MPa, tensile strength $f_{ct} = 2.25$ MPa, and modulus of elasticity $E_c = 36.7$ GPa. Furthermore, the GFRP bars used had a tensile strength $f_f = 809$ MPa and modulus of elasticity $E_f = 50$ GPa (Gomes et al., 2023).

With the data incorporated into the proposed model, the GRG method obtained a critical rotation equal to $2.619e-3$ rad and a neutral axis depth equal to 20.85 mm. The value of the objective function F evaluated at the optimal points was $3.232e-8$. The evaluation on equations R_1 and R_2 , led to a residual of $1.08e-4$ and $1.4e-4$, respectively.

The crack kinematics given from the obtained values of the critical rotation and the neutral axis depth is presented in Figure 6, and the crack opening-slip relationship obtained for the critical crack stage is shown in Figure 7.

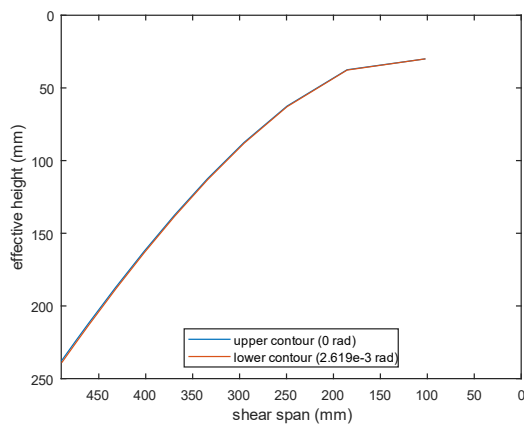


Figure 6: critical kinematics

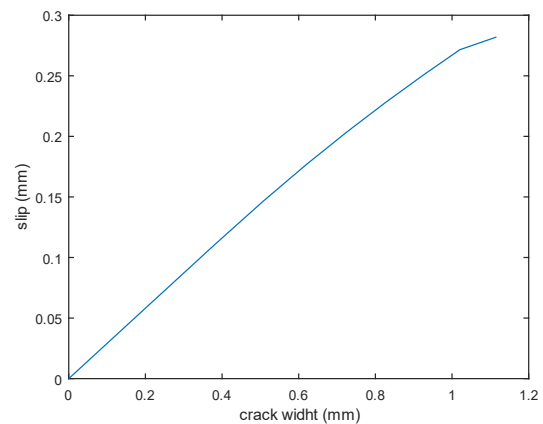


Figure 7: crack width-slip at rupture

The graphs in Figures 8 and 9 present the quantification of the transfer mechanisms in the shear strength and the flexural strength.

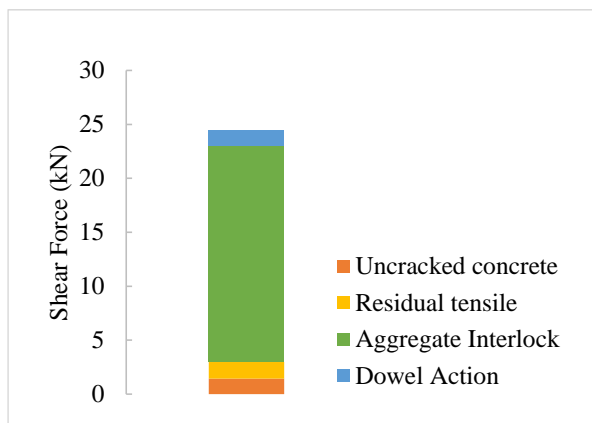


Figure 8: resistant shear at rupture

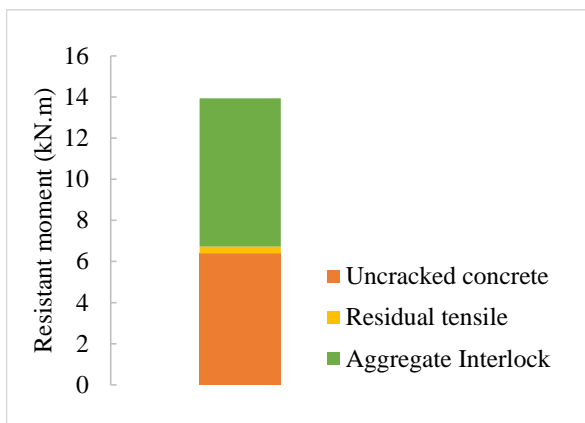


Figure 9: resistant moment at rupture

From Figure 8, it can be seen that the shear force resisted by the parcels of the uncracked concrete, the residual tension, the aggregate interlock, and the dowel action are 1.44 kN, 1.54 kN, 20.05 kN, and 1.54 kN, respectively, resulting in the shear capacity equal to 24.46 kN. For the moment strength (Figure 9), 6.39 kN.m is given by the uncracked concrete, 0.33 kN.m by the residual tensile stress in the concrete, and 7.21 kN.m is given by the aggregate interlock, resulting a moment strength of 13.94 kN.m.

CONCLUSIONS

The proposed model obtains the critical kinematics of the shear crack and, individually accounting the transfer mechanisms that contributes to the resistant capacity of the beam. The kinematics is obtained from the determination of the critical rotation and the depth of the neutral axis that leads to the equilibrium forces and moments in the section.

Based on the results, it was possible to observe that the proposed methodology was satisfactory since the algorithm adequately minimized the objective function, reaching reasonable values of rotation and depth of neutral axis for the physical problem. With the rotation value, the critical kinematics can be established and the actions evaluated.

The model was applied to reinforced concrete beams with GFRP bars and it was possible to quantify the contribution of each transfer mechanism in the failure. The results obtained showed that, for this application, the aggregate interlock was the dominant mechanism in failure.

CONFLICT OF INTEREST

The authors declare that they have no conflicts of interest associated with the work presented in this paper.

DATA AVAILABILITY

Data on which this paper is based is available from the authors upon reasonable request.

ACKNOWLEDGEMENT

This study was financed in part by the Coordenação de Aperfeiçoamento de Pessoal de Nível Superior – CAPES, Finance Code 001 – and in part by the Brazilian funding agencies FAPERJ and CNPq.

REFERENCES

- Abadie, J., & Carpentier, J. (1965). Généralisation de la Méthode du Gradient Réduit de Wolfe au cas des Contraintes Non Lineaires. *Proceedings IFORS Conference*.
- Baumann, T., & Rusch, H. (1970). Versuche zum stadium der verdubelungswirkung der biegezugbewehrung eines stahlbetonbalkens. *Deutscher Ausschuss Fur Stahlbeton, Heft 210*, 45–83.
- Bazant, Z. P., & Gambarova, P. G. (1980). Rough crack models in reinforced concrete. *ASCE – Journal of Structural Engineering*, 106(4), 819–842.
- Campana, S., Fernández Ruiz, M., Anastasi, A., & Muttoni, A. (2013). Analysis of shear-transfer actions on one-way RC members based on measured cracking pattern and failure kinematics. *Magazine of Concrete Research*, 65(6), 386–404. <https://doi.org/10.1680/macrc.12.00142>
- Cavagnis, F. (2017). Shear in reinforced concrete without transverse reinforcement: from refined experimental measurements to mechanical models. *Thesis*, 223.
- Cavagnis, F., Fernández Ruiz, M., & Muttoni, A. (2018a). A mechanical model for failures in shear of members without transverse reinforcement based on development of a critical shear crack. *Engineering Structures*, 157(February 2017), 300–315. <https://doi.org/10.1016/j.engstruct.2017.12.004>
- Cavagnis, F., Fernández Ruiz, M., & Muttoni, A. (2018b). An analysis of the shear-transfer actions in reinforced concrete members without transverse reinforcement based on refined experimental measurements. *Structural Concrete*, 19(1), 49–64. <https://doi.org/10.1002/suco.201700145>
- Classen, M. (2020). Shear Crack Propagation Theory (SCPT) – The mechanical solution to the riddle of shear in RC members without shear reinforcement. *Engineering Structures*, 210(December 2019), 110207. <https://doi.org/10.1016/j.engstruct.2020.110207>
- Costa, G., & Cardoso, D. C. T. (2023). Nonlinear Analysis of GFRP Reinforced Concrete Beams using Moment-Rotation Approach and Conjugate Beam Method. *Engineering Structures*, in press. <https://doi.org/10.1016/j.engstruct.2023.116499>
- Fenwick, R. C., & Paulay, T. (1968). Mechanisms of Shear Resistance of Concrete Beams. *Journal of the Structural Division*, 94(10), 2325–2350. <https://doi.org/10.1061/JSDEAG.0002092>
- Fernández Ruiz, M., & Muttoni, A. (2008). Shear strength in one- and two-way slabs according to the Critical Shear Crack Theory. In *Tailor Made Concrete Structures* (pp. 559–563). CRC Press. <https://doi.org/10.1201/9781439828410.ch92>
- FIB. (2014). *Model Code 2010 - Vol.1. 1*, 1–5.
- Gomes, T. A., de Resende, T. L., & Cardoso, D. C. T. (2023). Shear-transfer mechanisms in reinforced concrete beams with GFRP bars and basalt fibers. *Engineering Structures*, 289(May), 116299. <https://doi.org/10.1016/j.engstruct.2023.116299>
- H.P.J. Taylor. (1974). The fundamental behaviour of reinforced concrete beams in bending and shear. *Symposium Paper*, 42, 43–78.
- Hillerborg, A.; Modeer, M. . P. P.-E. . (1976). Analysis of crack formation and crack growth in concrete by means of fracture mechanics and finite element. *Cement and Concrete Research*, 6(6), 773–782.
- Hillerborg, A. (1980). Analysis of fracture by means of the fictitious crack model, particularly for fibre reinforced concrete. *The International Journal of Cement Composites*, 2(4), 177–184.
- Hognestad, E., Hanson, N. W., & McHenry, D. (1955). Concrete Stress Distribution in Ultimate Strength Design. *ACI Journal Proceedings*, 52(12), 455–480. <https://doi.org/10.14359/11609>
- Lasdon, L., Fox, R., & Ratner, M. (1974). Nonlinear optimization using the generalized. *Informatique et Recherche Opérationn*, 3, 73–103.
- Lasdon, L. S., Waren, A. D., Jain, A., & Ratner, M. (1978). Design and Testing of a Generalized Reduced Gradient Code for Nonlinear Programming. *ACM Transactions on Mathematical Software*, 4(1), 34–50. <https://doi.org/10.1145/355769.355773>
- Li, B., Maekawa, K., & Okamura, H. (1989). Contact density model for cracks in concrete. *IABSE Colloquium, Delft*, 54(February 1989), 51–62.
- Marí, A., Bairán, J., Cladera, A., Oller, E., & Ribas, C. (2015). Shear-flexural strength mechanical model for the design and assessment of reinforced concrete beams. *Structure and Infrastructure Engineering*, 11(11), 1399–1419. <https://doi.org/10.1080/15732479.2014.964735>
- Monserrat López, A., Fernández Ruiz, M., & Miguel Sosa, P. F. (2021). The influence of transverse

- reinforcement and yielding of flexural reinforcement on the shear-transfer actions of RC members. *Engineering Structures*, 234(December 2020), 111949. <https://doi.org/10.1016/j.engstruct.2021.111949>
- Muttoni, A., & Fernández Ruiz, M. (2008). Shear Strength of Members without Transverse Reinforcement as Function of Critical Shear Crack Width. *ACI Structural Journal*, 105(2), 103–118. <https://doi.org/10.14359/19731>
- Muttoni, A., & Schwartz, J. (1991). Behaviour of Beams and Punching in Slabs without Shear Reinforcement. *IABSE Colloquium*, 62, 703–708.
- Reineck K.-H. (1991). Ultimate Shear Force of Structural Concrete Members without Transverse Reinforcement derived from a Mechanical Model. *ACI Structural Journal*, 88(88), 592–602.
- Resende, T. L. de. (2020). *Contribuição dos mecanismos resistentes à força cortante em vigas de concreto armado sem e com fibras de aço (Tese de doutorado)*. Pontifícia Universidade Católica do Rio de Janeiro (PUC-Rio).
- Sacoman, M. A. R. (2021). *Otimização de projetos utilizando GRG, solver e excel*. <https://doi.org/10.37423/220105260>
- T. Paulay, & P.J. Loeber. (1974). Shear Transfer By Aggregate Interlock. *Symposium Paper*, 42, 1–16.
- Vintzēleou, E. N., & Tassios, T. P. (1986). Mathematical models for dowel action under monotonic and cyclic conditions. *Magazine of Concrete Research*, 38(134), 13–22. <https://doi.org/10.1680/mac.1986.38.134.13>
- Walraven, J. C. (1980). *Aggregate Interlock: A theoretical and experimental analysis*. University of Delft.
- Walraven, J. C., & Reinhardt, H. W. (1981). Theory and experiments on the mechanical behavior of cracks in plain and reinforced concrete subjected to shear loading. *Heron. Dept. of Civil Engineering, Delft University of Technology*, 26(1A), 68p.